





Demonstration of 24-hour continuous optical turbulence monitoring in a city

L. F. BEESLEY,^{1,2} R. GRIFFITHS,^{1,3}  K. HARTLEY,^{1,*} O. J. D. FARLEY,¹  F. QUATRESOOZ,⁴ A. RODRÍGUEZ-GÓMEZ,⁵ A. COMERÓN,⁵ M. TOWNSON,⁶  D. ALALUF,⁷ AND J. OSBORN¹ 

¹Centre for Advanced Instrumentation, Department of Physics, Durham University, Durham DH1 3LE, UK

²School of Metallurgy and Materials, University of Birmingham, Birmingham B15 2TT, UK

³Department of Physics, University of Oxford, Denys Wilkinson Building, Keble Road, Oxford OX1 3RH, UK

⁴ICTEAM Institute, Université Catholique de Louvain (UCLouvain), Louvain-la-Neuve, Belgium

⁵CommSensLab-UPC, Universitat Politècnica de Catalunya, Barcelona, Spain

⁶Northumbria University, Dept. Math, Physics, and Electrical Engineering, Ellison Pl., Newcastle upon Tyne, NE1 8ST, UK

⁷European Space Agency - ESA/ESTEC, Keplerlaan 1, NL-2200 AG Noordwijk, Netherlands

*kathryn.e.hartley@durham.ac.uk

Abstract: Atmospheric optical turbulence limits the performance of free-space optical communication links between the ground and space. The bandwidth provided by optical links enables the realization of ubiquitous, high-bandwidth and secure communications anywhere on Earth. However, currently very little is known about the nature and dynamics of vertical optical turbulence in critical urban environments, close to data centers and users that require high-bandwidth connections. TURBO is a turbulence monitoring facility, based on the 24-hour Shack-Hartmann Image Motion Monitor (24hSHIMM) instrument, capable of measuring optical atmospheric turbulence 24-hours a day in stronger turbulence conditions. Here we show a demonstration of continuous turbulence monitoring in an urban environment for the first time in Barcelona, Spain. TURBO will be an autonomous monitor generating valuable data for the community.

Published by Optica Publishing Group under the terms of the [Creative Commons Attribution 4.0 License](https://creativecommons.org/licenses/by/4.0/). Further distribution of this work must maintain attribution to the author(s) and the published article's title, journal citation, and DOI.

1. Introduction

Atmospheric optical turbulence is a key limiting factor in the performance of free-space optical communication systems. Therefore, it is important to understand the optical turbulence parameters at the locations of potential optical ground stations (OGSs). Previous studies attempt to estimate this information through the analysis of archival meteorological data and an assessment of the local environment's structure [1–5]. However, to ensure accuracy, such models require assimilation and validation with real measurements.

To address this need, we present TURBO (TURBulence mOnitoring and forecasting), a turbulence monitoring facility capable of providing 24-hour continuous turbulence measurements in an urban environment. TURBO, is installed within a dome on a building at the Universitat Politècnica de Catalunya (UPC) in Barcelona, Spain. TURBO will complement the array of permanent atmospheric instruments stationed at UPC, including sun photometers and an aerosol LIDAR [6]. These instruments will not only aid in understanding how aerosols can impact atmospheric turbulence but will also provide insights into the optical transmission through the atmosphere, in addition to turbulent effects.

Current atmospheric measurements are primarily focused on remote locations for astronomical applications or to study horizontal links [7,8]. However, there is a significant gap in research regarding the vertical atmospheric profiles of turbulence close to high-data users such as densely built-up urban areas or near data processing centers. Understanding these vertical pathways is crucial for the development and optimization of bi-directional satellite-to-ground optical links. Using TURBO, we aim to address this gap by presenting the first continuous day and night optical turbulence measurements in an urban environment.

In addition to turbulent losses, gases, aerosols, and particulates can contribute to atmospheric attenuation through scattering and absorption. For satellite-to-ground optical links, cloud cover is a key contributor to this signal loss, causing fading and potentially a complete loss of signal [9–11]. Furthermore, in an urbanized environment, air pollutants such as dust and black carbon are prevalent and require adequate characterization to understand their impact on FSOC performance [12].

In this study, we present 40 hours of continuous data of the Fried parameter, r_0 , Rytov variance, σ_R^2 , isoplanatic angle, θ_0 and coherence time, τ_0 , measured using TURBO. These parameters can be used to quantify turbulence-induced signal degradation in a communication link. Specifically, r_0 describes wavefront aberrations at the receiver, which can cause poor fibre-optic coupling in coherent detection schemes [13]. σ_R^2 measures the intensity fluctuations, or scintillation, that result in signal loss. θ_0 and τ_0 measure the angular and temporal coherence of atmospheric turbulence, respectively. These parameters determine the rate at which wavefront aberrations need to be corrected and indicate the reciprocity between the downlink and uplink channel, which can be used to characterize the suitability of uplink correction techniques such as precompensation [14–16].

This paper also presents the culmination of 70 hours of measurements taken over different seasons, which are used to build an initial statistical analysis of the site.

The intention of this paper is to introduce TURBO to the community as a unique and novel facility demonstrating continuous measurement of vertical optical turbulence, 24-hours a day, in a relevant environment for FSOC (i.e., in a city), serving as a valuable data source for the FSOC research community. Data will be published periodically and interest in this data can be registered with the authors.

2. Barcelona as a site for OGS studies

Cloud cover is a primary contributor to signal loss and requires careful consideration when deciding the placement of an OGS. Barcelona lies in the northwest of Spain along the Mediterranean coast and as such has typically clear weather conditions. Figure 1 shows the average fractional cloud cover for 2022. Consequently, the mean downtime of an optical system during this period will be 28% from cloud coverage alone. This map highlights that Barcelona experiences some of the clearest weather conditions in Europe, making it an optimal location for an OGS.

The typical aerosols that are found in Barcelona are urban including "big" particles PM_{2.5} and PM₁₀, marine, frequent episodes of Saharan dust and frequent episodes of burnt biomass. High levels of traffic gaseous pollutants have been measured at urban ground monitoring sites and layers of tropospheric ozone have been recorded at lower levels [17]. These aerosols in the atmosphere cause scattering or absorption of propagating photons, leading to signal loss and a reduction in the performance of optical links [18]. The data provided by UPC's instruments at the site is invaluable for understanding the distribution and impact of these aerosols, providing insights into the characteristics of the communication medium.

Additionally, as a Mediterranean city, Barcelona serves as a representative site for the region. This is particularly significant because Marseille, also a Mediterranean city, hosts a submarine fibre-optic landing site making it the central hub for data traffic between Europe, the Middle East and North Africa region, and Asia [19].

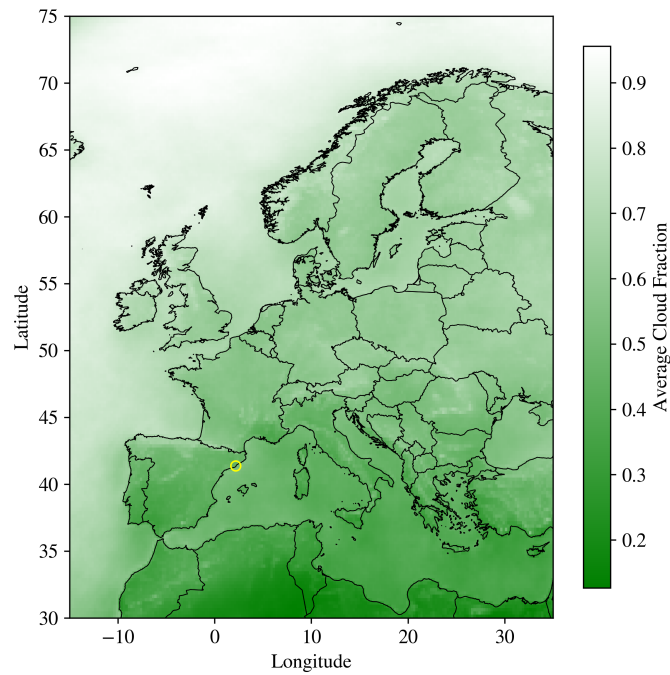


Fig. 1. Map of average cloud fraction over Europe for 2022. The location of Barcelona, with a cloud fraction value of 0.29, is marked with a yellow circle. The data is from the CLARA-A3 dataset provided by EUMETSAT.

3. Instrument

TURBO utilizes a small (28 cm diameter) commercial telescope and 24-hour Shack-Hartmann Image Motion Monitor (SHIMM) for optical turbulence monitoring. The 24hSHIMM uses a Shack-Hartmann wavefront sensor to measure a 4-layer vertical optical turbulence profile. From this, r_0 , σ_R^2 , θ_0 and τ_0 , are calculated. 24hSHIMM observes stars in the short-range infra-red (with a bandpass of 900-1700 nm) to reduce sky background intensity during the daytime. For further details on the 24hSHIMM see [20].

The instrument has been cross-validated against established turbulence profiling instruments during the night in [21] and via Monte-Carlo wave-optical simulations. Daytime cross-validation experiments are yet to be made as daytime turbulence monitors are comparatively far less common. However, its performance has been validated through simulations that incorporate realistic levels of daytime noise as in [20]. For TURBO, the SHIMM body has been redesigned for long-term durability, which uses an aluminium case to prevent movement of the optics caused by gravity as the telescope slews. The unit is also sealed to prevent dust and moisture from contaminating the optics. An annotated 3D model of the updated design can be found in Fig. 2.

TURBO will be installed indefinitely at UPC to gather long-term statistics. It is fixed to a metal pier to maintain telescope alignment and minimize vibrations. The instrument is then housed within a ScopeDome 3M clamshell dome to protect it from adverse weather. An Oculus PRO 180-degree all-sky camera has been installed alongside a Vaisala WTX 536 weather station (seen in Fig. 3) which will enable automatic opening and closing of the dome to allow data collection whenever there are clear skies. In addition, the weather data, such as the temperature, wind speed and direction, can be compared to the measured atmospheric turbulence profiles to determine correlated behavior.

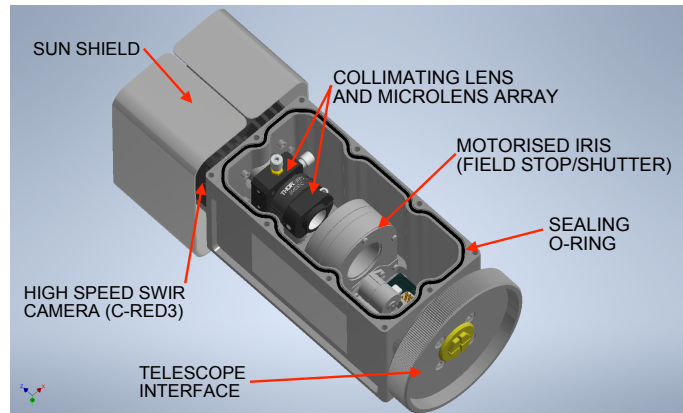


Fig. 2. A 3D model of the updated opto-mechanical design for the 24hSHIMM used for TURBO.



Fig. 3. Image of TURBO instruments on the roof of UPC. The all-sky camera and weather sensor are on the left, while TURBO1 is enclosed within the dome on the right.

4. Demonstration of continuous optical turbulence measurements

This section provides a demonstration of TURBO, with the expectation that future data accumulation will allow for a more comprehensive statistical analysis of the site. All results presented in this section are scaled to a reference wavelength of 500 nm.

Figure 4 presents the results of continuous measurements from our commissioning campaign which were taken over 40 hours. To the best of our knowledge, this is the first continuous optical turbulence measurements taken in an urban environment that includes both daytime and nighttime measurements. There are gaps in the data partway through the second night of measurements, attributed to high winds shaking the star out of the field of view which interrupts auto-guiding. All measurements presented here are scaled to zenith and a wavelength of 500 nm.

The turbulent data measured in Fig. 4 exhibits fluctuations over comparable time scales. Over the 40-hours, measured parameters seem to be independent of day or night time conditions with the most significant changes seen in the transition between night and day. Additionally, in each dataset, it is observed that the optical turbulence became much weaker towards 18:00 of each day, as the sun began to set. This pattern has been documented and observed (see [22]) and is attributed to a reduced temperature gradient between the boundary layer and the ground leading to reduced convection.

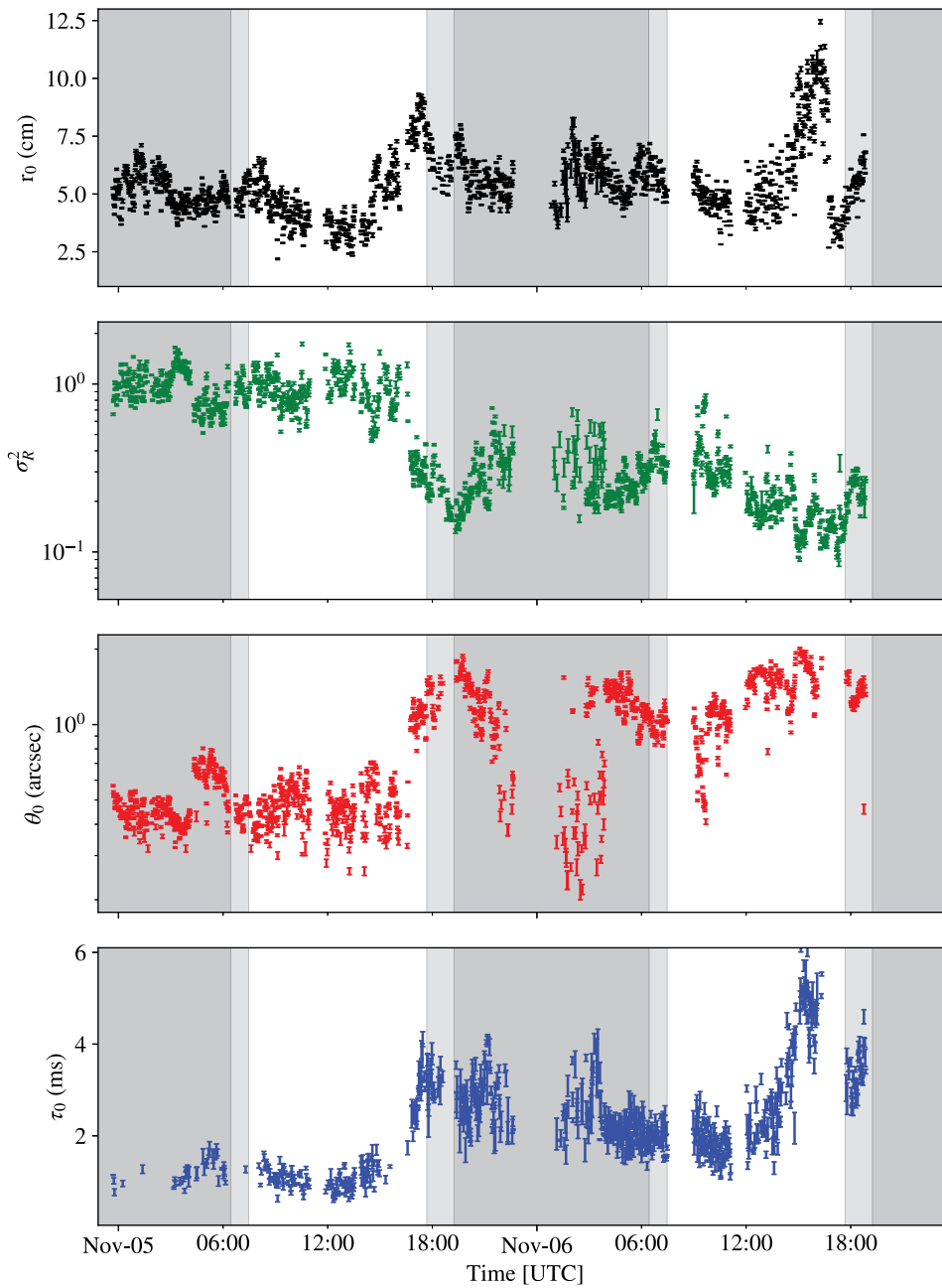


Fig. 4. Measured turbulence parameters over 40 hours in Barcelona, Spain. The panels represent (from top to bottom): r_0 , σ_R , θ_0 , and τ_0 , all scaled to zenith and to a wavelength of 500 nm. The white, light grey and dark grey shading corresponds to daytime, twilight periods and nighttime, respectively.

The wind speeds of the available atmospheric layers, from ECMWF ERA5 data, are presented in Fig. 5 for comparison with the observed turbulent conditions. The strong wind layer observed at approximately 15 km aligns with the typical altitude range of jet streams [23]. Both high- and low-altitude wind speeds during the first 12 hours are significantly higher than at any other time during the experiment, leading to elevated turbulence parameters during this period, as shown in Fig. 4. Following this period, wind speeds at both altitudes gradually decreased. These measurements were taken toward the end of Storm Ciarán as it was passing through Europe, which may explain the high wind speeds observed.

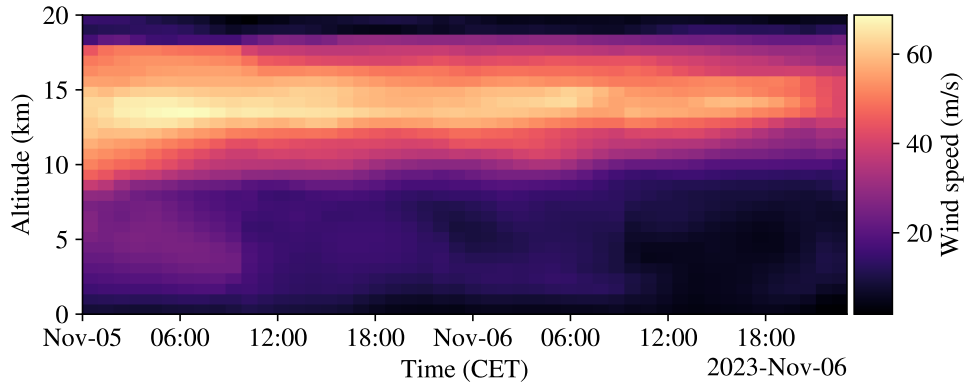


Fig. 5. Wind speed as a function of altitude and time. Data sourced from the ECMWF ERA5 reanalysis dataset.

In summary, the measured turbulence conditions observed at UPC, Barcelona, exhibit large temporal fluctuations. To a first degree, the strength of the turbulent effects appears to correlate with the atmospheric wind speeds and with the diurnal cycle. The sequences demonstrate a complex dynamic in the variation of the measured parameters.

5. Statistical analysis of site

As of July 2024, TURBO1 has collected over 70 hours of measurements, equalling 6,500 data points. This data was collected during three campaigns: November 2023, February 2024, and May 2024, enabling us to begin to develop a preliminary statistical understanding of the turbulent parameters at this location.

Figures 6 show histograms for the Fried parameter, Rytov index, isoplanatic angle, and coherence time. The data is divided into day and night datasets, where day is defined as the time between sunrise and sunset, and night is the time between sunset and sunrise, specific to each respective time of year. Table 1 summarizes the statistics of these histograms, providing the median, first quartile (Q1), and third quartile (Q3) for each turbulent parameter.

Table 1. Summary statistics for turbulent parameters. All parameters are scaled to 500 nm.

Parameter	Day			Night		
	Median	Q1	Q3	Median	Q1	Q3
r_0 (cm)	4.9	3.9	7.0	6.2	5.2	7.7
σ_R^2	0.25	0.18	0.42	0.26	0.18	0.40
θ_0 (arcsec)	1.1	0.79	1.5	1.1	0.81	1.5
τ_0 (ms)	2.7	1.8	4.0	2.9	1.8	5.9

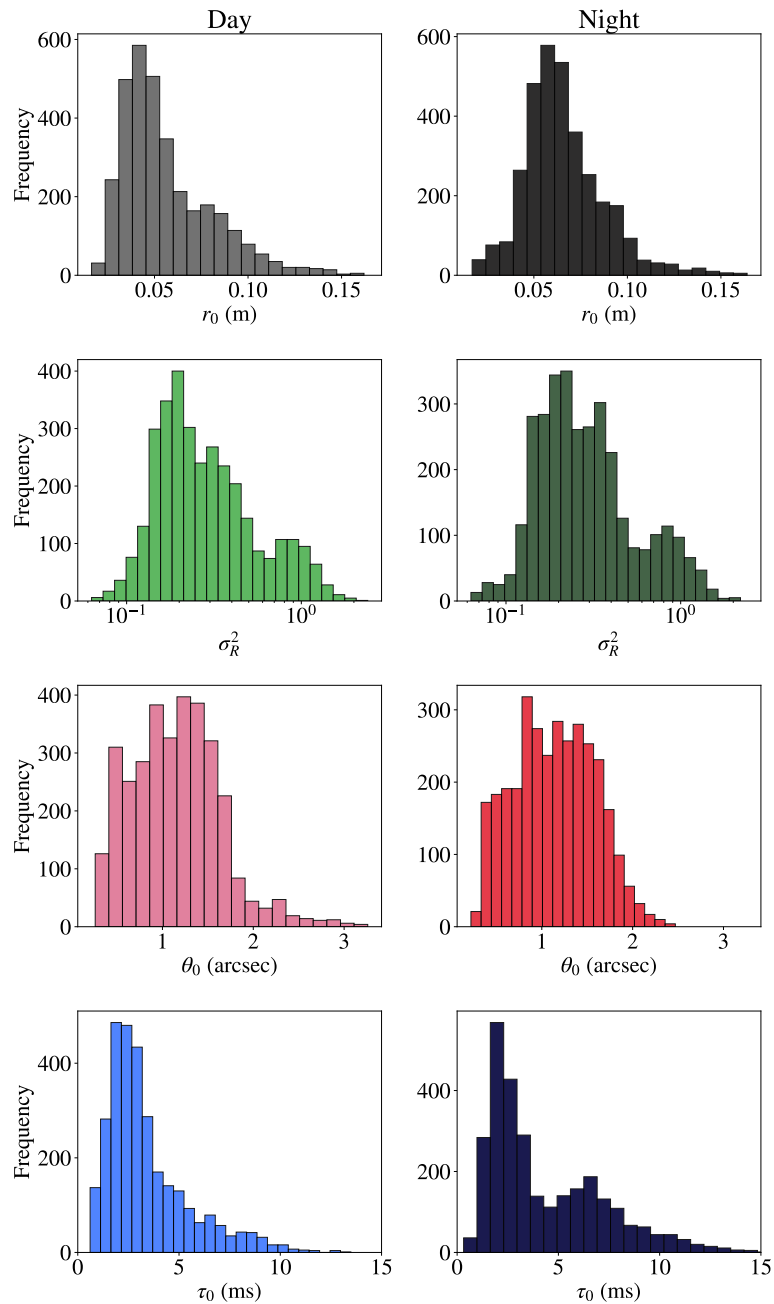


Fig. 6. Histograms of turbulent parameters during day and night. The rows correspond to different turbulent parameters: r_0 , σ_R^2 , θ_0 , and τ_0 from top to bottom. The columns represent different time periods: day and night from left to right. Each histogram shows the frequency distribution of the respective parameter values for the specified time period, where each row shares the same x-axis.

From these observations, several trends can be identified. The median Fried parameter (r_0) is 4.9 cm during the day and 6.2 cm at night. By contrast, astronomical sites generally record r_0 values nearer to 10–20 cm under typical conditions, with some reaching upwards of 20 cm in ideal conditions. Notably, 25% of the nighttime data shows r_0 values larger than 7.7 cm, suggesting slightly better seeing conditions at night compared to the day. However, even during the daytime, the median r_0 remains at 4.9 cm, indicating that the turbulence is not as strong as predicted by some models, which might have anticipated worse conditions. Since daytime studies require an optical source, the most accessible way to obtain daytime turbulence measurements is through horizontal measurements, as demonstrated in studies like [24–27]. These cases typically involve long propagation paths through ground layer turbulence, resulting in a large integrated turbulence strength where r_0 can reach the millimetre scale. The values presented here align with horizontal measurements over shorter distances such as those seen in [28].

σ_R^2 remains consistent between day and night, with median values being 0.25 and 0.26, respectively, representing moderately strong turbulence. This is supported by the similar interquartile ranges, suggesting a very small variance between day and night. This aligns with the continuous dataset shown in Fig. 4 where the most significant change in the σ_R^2 was in the transition from day to night. As σ_R^2 is weighted to turbulence away from the receiver (ie higher altitude turbulence) it is not surprising that it has less diurnal variation than r_0 which is dominated by low-altitude turbulence and is driven by solar heating of the ground.

The median θ_0 is 1.1 arcseconds for both day and night conditions. For FSOC, the uplink beam must be aimed slightly ahead of the satellite's current position due to the satellite's relative motion and the time taken for the light to travel between the transmitter and receiver. This offset, known as the point-ahead angle, ensures that the beam reaches the satellite's location at the time of reception. This angle is 4 arcseconds for communications with GEO satellites. Since this value is greater than the measured median at Barcelona we can say that the downlink and uplink channels are weakly correlated, indicating that precompensation may fail when using the phase from the downlink beam [29]. Alternative methods of turbulence compensation, such as using a laser guide star or phase estimation, may need to be explored [16,30].

Similarly, τ_0 remains relatively stable between day and night with the median lying at 2.7 ms and 2.9 ms, respectively. This parameter is useful for understanding the rate at which the optical system must correct for atmospheric turbulence. Median τ_0 values for astronomical sites are around 4 ms, representing the best possible turbulent conditions [31]. Given the more challenging environment, the values observed here are quite reasonable.

6. Conclusion

This paper presents the commissioning of TURBO, a state-of-the-art turbulence monitoring facility which is designed to provide continuous, 24-hour turbulence data to aid in characterising atmospheric turbulence in Barcelona. TURBO operates within a dome, with plans for full automation to facilitate data collection during clear sky conditions. The data gathered can be used to validate turbulence forecast models in urban environments, aid in the optical design of a communication link, and to simulate FSOC performance under realistic turbulence conditions.

The first continuous day and night optical turbulence measurements taken in an urban environment are presented, with each value being scaled to a reference wavelength of 500 nm. The data demonstrates that turbulence levels can fluctuate over a wide range in short timescales, such as r_0 evolving from 3 cm to 12 cm within 3 hours. The measured σ_R^2 is observed to fluctuate between strong and moderate turbulence over this dataset. Additionally, it was observed that turbulence strength decreases during the transition through sunset.

We also provide a preliminary statistical analysis of the turbulent parameters based on over 70 hours of measurements collected across three campaigns. The data shows that nighttime conditions generally offer slightly better seeing, with a median Fried parameter of 6.2 cm

compared to 4.9 cm during the day. The Rytov variance, isoplanatic angle, and coherence time all remain relatively stable regardless of daytime or nighttime conditions, which we believe is due to these variables being primarily influenced by high-altitude turbulence, which fluctuates less with solar heating.

Future work will use continuous data from the measurements of TURBO to help perform site characterization. UPC's vertical LIDAR can be used in combination with atmospheric optical turbulence measurements for a more comprehensive understanding of the environment. This will enable the assessment of the feasibility of establishing an optical ground station within Barcelona or sites with similar meteorological properties. The data will also be used to develop optical turbulence modelling and forecast tools through validation and assimilation opportunities.

Once autonomous operation is developed and tested the system can be replicated elsewhere to provide the community with critical optical turbulence measurements in relevant environments.

Funding. Engineering and Physical Sciences Research Council (EP/T518001/1); UK Research and Innovation (MR/X015106/1); European Space Agency (4000140195/22/NL/MM/fm).

Acknowledgments. The results presented in this paper make use of NumPy [32], Matplotlib [33], Python [34], Pandas [35], EUMETSAT's CLARA-5 data [36] and ECMWF's ERA5 data [37].

Disclosures. The authors declare no conflicts of interest.

Data availability. Data underlying the results presented in this paper are not publicly available at this time but may be obtained from the authors upon reasonable request.

References

1. E. Masciadri, F. Lascaux, A. Turchi, *et al.*, "Optical turbulence forecast: Ready for an operational application," *Mon. Not. R. Astron. Soc.* **466**(1), 520–539 (2017).
2. J. Osborn and M. Sarazin, "Atmospheric turbulence forecasting with a general circulation model for Cerro Paranal," *Mon. Not. R. Astron. Soc.* **480**(1), 1278–1299 (2018).
3. E. Masciadri, A. Turchi, and L. Fini, "Towards operational optical turbulence forecast systems at different scales," in *Adaptive Optics Systems VIII* p. 61 (2023).
4. F. Quatresooz, R. Griffiths, L. Bardou, *et al.*, "Continuous daytime and nighttime forecast of atmospheric optical turbulence from numerical weather prediction models," *Opt. Express* **13**(3), 1282 (2023).
5. A. Y. Shikhovtsev, P. G. Kovadlo, A. A. Lezhenin, *et al.*, "Influence of Atmospheric Flow Structure on Optical Turbulence Characteristics," *Opt. Express* **31**(21), 33850 (2023).
6. S. Lolli, M. Sicard, F. Amato, *et al.*, "Climatological assessment of the vertically resolved optical and microphysical aerosol properties by lidar measurements, sun photometer, and in situ observations over 17 years at Universitat Politècnica de Catalunya (UPC) Barcelona," *Atmos. Chem. Phys.* **23**(19), 12887–12906 (2023).
7. M. Schöck, S. Els, R. Riddle, *et al.*, "Thirty Meter Telescope Site Testing I: Overview," *Publ. Astron. Soc. Pac.* **121**(878), 384–395 (2009).
8. Y. Jiang, J. Ma, L. Tan, *et al.*, "Measurement of optical intensity fluctuation over an 11.8 km turbulent path," *Opt. Express* **16**(10), 6963 (2008).
9. S. Piazzolla and S. Slobin, "Statistics of link blockage due to cloud cover for free-space optical communications using NCDC surface weather observation data," in *Free-Space Laser Communication Technologies XIV*, vol. 4635 G. S. Mecherle, eds. (2002), pp. 138–149.
10. S. Poulenard, M. Ruellan, B. Roy, *et al.*, "High altitude clouds impacts on the design of optical feeder link and optical ground station network for future broadband satellite services," *Free-Space Laser Communication and Atmospheric Propagation XXVI* **8971**, 897107 (2014).
11. M. Birch, J. R. Beattie, F. Bennet, *et al.*, "Availability, outage, and capacity of spatially correlated, Australasian free-space optical networks," *J. Opt. Commun. Netw.* **15**(7), 415 (2023).
12. I. I. Kim, B. McArthur, and E. J. Korevaar, "Comparison of laser beam propagation at 785 nm and 1550 nm in fog and haze for optical wireless communications," in *Optical Wireless Communications III*, vol. 4214 E. J. Kim, eds. (2001), pp. 26–37.
13. A. Belmonte, A. Rodríguez, F. Dios, *et al.*, "Phase compensation considerations on coherent free-space laser communications system," (2007), p. 67361A.
14. R. Tyson and J. Love, *Principles of Adaptive Optics* (Elsevier, 1991).
15. A. Montmerle-Bonnefois, C. Petit, C. B. Lim, *et al.*, "Adaptive optics precompensation of a GEO feeder link: The FEDELIO experiment," *Optics InfoBase Conference Papers, Part F149-*, 1–8 (2019).
16. R. Biasi, D. Bonaccini Calia, M. Centrone, *et al.*, "ALASCA: the ESA Laser Guide Star Adaptive Optics Optical Feeder Link demonstrator facility," in *International Conference on Space Optics - ICSO 2022*, vol. 12777 K. Minoglou, N. Cugny, and B. Centrone, eds. (SPIE, 2023), p. 186.

17. M. Dall'Osto, X. Querol, A. Alastuey, *et al.*, "Presenting SAPUSS: Solving aerosol problem by using synergistic strategies in Barcelona, Spain," *Atmos. Chem. Phys.* **13**(17), 8991–9019 (2013).
18. H. Ding, B. M. Sadler, G. Chen, *et al.*, "Modeling and characterization of ultraviolet scattering communication channels," in *Advanced Optical Wireless Communication Systems*, vol. 9780521197 (Cambridge University Press, 2012), pp. 177–200.
19. J.-P. Larçon and C. Vadcar, "EU-Asia Connectivity: France's Three Largest Cities and China's Belt and Road," *China and the World* **03**(01), 2050001 (2020).
20. R. Griffiths, J. Osborn, O. Farley, *et al.*, "Demonstrating the first 24-hour continuous vertical monitoring of the atmospheric optical turbulence," *Opt. Express* **31**(4), 6730–6740 (2023).
21. R. Griffiths, L. Bardou, T. Butterley, *et al.*, "A comparison of next-generation turbulence profiling instruments at Paranal," *Mon. Not. R. Astron. Soc.* **529**(1), 320–330 (2024).
22. R. E. Good, R. R. Beland, E. A. Murphy, *et al.*, "Atmospheric Models Of Optical Turbulence," in *International Conference on Communications* (IEEE, 2015), 1988, p. 165.
23. F. K. Lutgens, *The Atmosphere: An Introduction to Meteorology* (2013), 12th ed.
24. B. M. Levine, E. A. Martinsen, A. Wirth, *et al.*, "Horizontal line-of-sight turbulence over near-ground paths and implications for adaptive optics corrections in laser communications," *Appl. Opt.* **37**(21), 4553 (1998).
25. L. C. Andrews, R. L. Phillips, D. Wayne, *et al.*, "Near-ground vertical profile of refractive-index fluctuations," *Atmospheric Propagation VI* **7324**, 732402 (2009).
26. A. V. Sergeev and M. C. Roggemann, "Monitoring the statistics of turbulence: Fried parameter estimation from the wavefront sensor measurements," *Appl. Opt.* **50**(20), 3519–3528 (2011).
27. L. Jiang, T. Dai, X. Yu, *et al.*, "Analysis of scintillation effects along a 7 km urban space laser communication path," *Appl. Opt.* **59**(27), 8418 (2020).
28. G. D. Love, C. N. Dunlop, S. Patrick, *et al.*, "Horizontal turbulence measurements using SLODAR," in *Atmospheric Optical Modeling, Measurement, and Simulation*, vol. 5891 S. M. Doss-Hammel and A. Kohnle, eds. (2005), p. 589104.
29. N. Martínez, L. F. Rodríguez-Ramos, and Z. Sodnik, "Toward the uplink correction: application of adaptive optics techniques on free-space optical communications through the atmosphere," *Opt. Eng.* **57**(07), 1 (2018).
30. P. Lognoné, J.-M. Conan, G. Rekaya, *et al.*, "Two-aperture measurements for GEO-feeder adaptive optics pre-compensation optimization," *Opt. Lett.* **48**(17), 4550 (2023).
31. M. Sarazina and A. Tokovinin, "The statistics of isoplanatic angle and adaptive optics time constant derived from DIMM data," *European Southern Observatory Conference and Workshop Proceedings* **58**, 1–8 (2001).
32. C. R. Harris, K. J. Millman, S. J. van der Walt, *et al.*, "Array programming with NumPy," *Nature* **585**(7825), 357–362 (2020).
33. J. D. Hunter, "Matplotlib: A 2D Graphics Environment," *Comput. Sci. Eng.* **9**(3), 90–95 (2007).
34. G. Van Rossum and F. L. Drake, *Python 3 Reference Manual* (CreateSpace, 2009).
35. W. McKinney, "Data Structures for Statistical Computing in Python," in *Proceedings of the 9th Python in Science Conference*, vol. 1 (2010), pp. 56–61.
36. K. G. Karlsson, M. Stengel, J. F. Meirink, *et al.*, "CLARA-A3: The third edition of the AVHRR-based CM SAF climate data record on clouds, radiation and surface albedo covering the period 1979 to 2023," *Earth Syst. Sci. Data* **15**(11), 4901–4926 (2023).
37. J. Muñoz-Sabater, E. Dutra, A. Agustí-Panareda, *et al.*, "ERA5-Land: A state-of-the-art global reanalysis dataset for land applications," *Earth Syst. Sci. Data* **13**(9), 4349–4383 (2021).